Optical properties of a semiconductor quantum dot with a single magnetic impurity: photoinduced spin orientation

Alexander O. Govorov[1] and Alexander V. Kalameitsev[2]
[1]*Department of Physics and Astronomy, Condensed Matter and Surface Science Program, Ohio University, Athens, Ohio 45701-2979, USA*
[2]*Institute of Semiconductor Physics, Novosibirsk, 630090 Russia*
(Received 27 September 2004; published 26 January 2005)

We describe the optical resonant manipulation of a single magnetic impurity in a self-assembled quantum dot. We show that using the resonant pumping one can address and manipulate selectively individual spin states of a magnetic impurity. The mechanisms of resonant optical polarization of a single impurity in a quantum dot involve anisotropic exchange interactions and are different than those in diluted semiconductors. A Mn impurity can be prepared in a given spin state and can act as qubit. The limiting factors for the spin manipulation are the electron-hole exchange interaction and finite temperature.

DOI: 10.1103/PhysRevB.71.035338 PACS number(s): 78.67.Hc, 42.50.Ct, 75.75.+a

I. Introduction

The spins of electrons in semiconductors strongly couple with electric and magnetic fields due to the spin-orbit and exchange interactions. Spintronics and quantum computation utilize these interactions to manipulate the electron spins.[1,2] One important class of spintronics materials is diluted magnetic semiconductors[3] which combine high quality semiconductor structures with magnetic properties of impurities. Since many semiconductors efficiently emit and absorb light, the spin states of electrons and magnetic impurities can be manipulated optically by using circularly polarized light pulses.[4] In diluted magnetic semiconductors such as bulk crystals, quantum wells, and dots, photogenerated excitons interact with a large collection of spins of Mn impurities and therefore a large number of degrees of freedom becomes involved.[5–11] In these systems, it is challenging to address individual spins of Mn atoms. At the same time, the quantum computational schemes are based on qubits, pairs of well-controlled quantum states. These elementary blocks, qubits, should be made interacting or decoupled on demand. In a diluted magnetic semiconductor, even a single Mn atom has six spin states ($I_{Mn}=5/2$). Therefore 15 different pairs of states (qubits) can be defined for a single Mn impurity. In addition, a single Mn impurity can act as two qubits which involve four out of six spin states. Here we study a system which allows us to manipulate optically a single Mn spin. This system is composed of a quantum dot (QD) and a single Mn impurity. We note that several physical aspects of a QD with a single Mn impurity were recently discussed in Refs. 12 and 13.

This paper describes a single Mn impurity embedded into a self-assembled QD. Importantly, such a system permits efficient selective optical control and manipulation of individual spin states and defining a single qubit for the Mn impurity. This ability comes from the exciton spectrum of a QD with a Mn atom. An exciton in a QD has a well-defined discrete spectrum and, simultaneously, strongly interacts with the Mn spin via the exchange interaction. Since the exciton and Mn spin functions become strongly mixed, the resonant optical excitation strongly affect the spin state of Mn impurity. In particular, we show that one can *write* spin states of an Mn atom. Since spin relaxation of paramagnetic ions in the absence of carriers (i.e., after the exciton recombination) is an extremely slow process ($\sim 10-100\ \mu$s), a single Mn spin is a very promising candidate for spintronics applications. The mechanisms of Mn-spin polarization in a QD are qualitatively different than those in bulk materials because of the discrete character of quantum states. In bulk, the photogenerated spin-polarized electrons transfer their spin to the Mn atoms or induce an effective magnetic field which polarizes the impurity system.[7] In a QD, the spin orientation of Mn atom comes from the three-body interactions involving an electron, hole, and Mn spin. The ability to manipulate a pair of chosen states (qubit) comes from the resonant excitation of a certain spin state of the exciton-Mn system. In addition, we describe the specific optical signatures of a Mn atom embedded into a QD. In contrast to the undoped self-assembled quantum dots, the optical emission of a laterally asymmetric quantum dot becomes *circularly polarized* due to the exciton-Mn interaction.

II. Model

We now consider a model of disk-shaped self-assembled QD taking into account only the heavy-hole (HH) states in the valence band. The QD potential strongly confines the electron and HH envelope wave functions $\phi_e(\mathbf{r}_e)$ and $\phi_h(\mathbf{r}_h)$ and the exchange interactions in the exciton determine the spin state of exciton. According to the conventional model, the Mn-hole and Mn-electron exchange interactions are proportional to $\delta(\mathbf{r}_{e(h)}-\mathbf{R}_{Mn})$, where $\mathbf{R}_{Mn}$ is the Mn position and $\mathbf{r}_{e(h)}$ is the electron (hole) coordinate. Then, the spin Hamiltonian takes the form

$$\hat{H}_{spin}=\hat{H}^{exc}_{Mn-hole}+\hat{H}^{exc}_{Mn-e}+\hat{H}^{exc}_{e-hole}, \tag{1}$$

which includes three types of exchange interaction. The anisotropic exchange interaction between the Mn spin and HH is $\hat{H}^{exc}_{Mn-hole}=(\beta/3)|\phi_h(\mathbf{R}_{Mn})|^2\hat{j}_{h,z}\hat{I}_{Mn,z}=A_h\hat{j}_{h,z}\hat{I}_{Mn,z}$; the Mn-

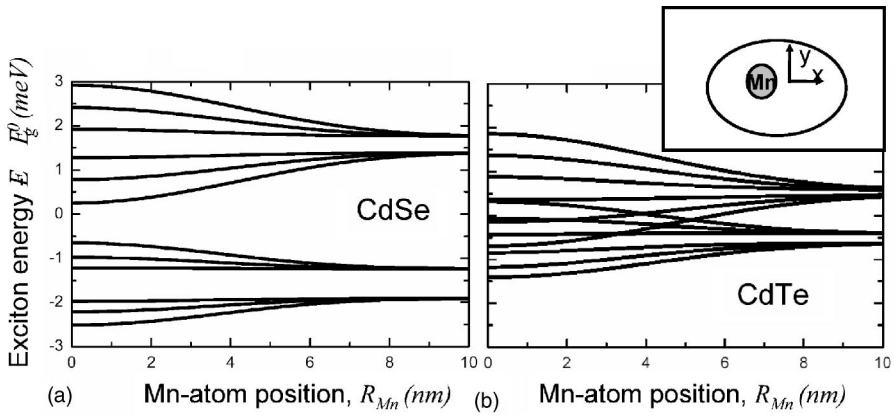

FIG. 1. Exciton energy spectrum as a function of the x coordinate of the Mn atom; $R_{Mn,y}=0$ and $R_{Mn,z}=L_z/2$. The energy E_g^0 is the band gap of a QD. (a) corresponds to $b_x=-0.7$, $b_y=-0.2$, $b_z=-0.4$, and $a_z=-1.2$ meV; (b) corresponds to −0.23, −0.066, −0.4, and −0.13 meV. Inset: geometry of the system.

electron interaction is isotropic, $\hat{H}^{exc}_{Mn-e}=\alpha|\phi_e(\mathbf{R}_{Mn})|^2\hat{\mathbf{s}}\hat{\mathbf{I}}_{Mn}=A_e\hat{\mathbf{s}}\hat{\mathbf{I}}_{Mn}$. Here, $\hat{\mathbf{I}}_{Mn}$ and $\hat{\mathbf{s}}$ are the Mn and electron spins, respectively ($s=1/2$, $I_{Mn}=5/2$); $\hat{\mathbf{j}}$ is the HH momentum ($j_h=3/2$ and $j_{h,z}=\pm 3/2$). The anisotropic e-HH interaction is given by the operator[14]

$$\hat{H}^{exc}_{e-hole}=\sum_{i=x,y,z} a_i\hat{j}_i\hat{s}_i+b_i\hat{j}_i^3\hat{s}_i, \tag{2}$$

where a_i and b_i are constants. The eigenstates of the Hamiltonian (1) are linear combinations of 24 functions, $|I_{Mn,z},j_{h,z},s_{e,z}\rangle$, where $I_{Mn,z}$, $j_{h,z}$, and $s_{z,e}$ are the z components of the corresponding momenta.

The strength of the Mn-hole and Mn-electron exchange interaction depends on the position of the Mn impurity with respect to the QD (Fig. 1, inset) and is given by the coefficients A_h and A_e. For the parameters of exchange interaction, we choose $\alpha N_0=0.29$ eV and $\beta N_0=-1.4$ eV, typical numbers for II-VI materials;[9,12] here N_0 is the number of cations for unit volume. In Fig. 1, we show the calculated spectrum of exciton as a function of the Mn position for two sets of parameters a_i and b_i. The first set [Fig. 1(a)] relates to the case of CdSe QD,[15] and the second [Fig. 1(b)] corresponds to the weaker e-hole exchange interaction and to a CdTe QD. For the QD wave function, we use a convenient approximation: $\phi_{e(h)}(\mathbf{r})=B_{e(h)}\sin(\pi z/L_z)e^{-x^2/l^2_{x,e(h)}-y^2/l^2_{y,e(h)}}$.[16,17] The sizes of QD's are $l_{x,e}=l_{x,h}=6$ nm, $l_{y,e}=l_{y,h}=4$ nm, and $L_z=2$ nm. In Fig. 1, we observe that, in the limit $R_{Mn}\to\infty$, a QD has a spectrum determined by the laterally anisotropic e-hole exchange interaction; the photoluminescence (PL) spectrum in this case is linearly polarized along the X and Y directions.[15] For the case $R_{Mn}\sim l_{dot}$, the energy structure strongly changes due to the Mn-induced exchange interaction that has cylindrical, D_{2d} point-group symmetry. This cylindrical symmetry results in the nonzero spin polarization of the wave functions.

The excitonic wave functions $|\gamma\rangle$ of energies E_γ ($\gamma=1,2,\ldots 24$) are doubly degenerate (Fig. 1) and their energy spectrum consists of 12 energy levels, $n=1,2,\ldots 12$ [Fig. 3(b)]. Wave functions in a pair of degenerate states can be written using the two noncrossing subspaces. For example, the states $|1\rangle(|2\rangle)$ are composed of wave functions with $I_{Mn,z}+j_{h,z}+s_{e,z}=2m+1/2$ $\quad(I_{Mn,z}+j_{h,z}+s_{e,z}=2m+1+1/2)$, where m is integer.

III. Master equation

The pumping and PL processes are described by the master equation

$$\frac{\partial\hat{\rho}}{\partial t}=\frac{i}{\hbar}[\hat{\rho},\hat{H}_0+\hat{V}_{opt,+}(t)]+L(\hat{\rho}), \tag{3}$$

where $\hat{\rho}$ is the density matrix, $\hat{V}_{opt,+}(t)=W_0(\hat{p}_+e^{i\omega_l t}+\hat{p}_-e^{-i\omega_l t})$ is the interaction with classical circularly polarized light, $\hat{p}_\pm=\hat{p}_x\pm i\hat{p}_y$, and ω_l is the laser frequency. $L(\hat{\rho})$ is the relaxation operator within the Markovian approximation:

$$[L(\hat{\rho})]_{\gamma,\gamma'}=-\frac{\Gamma_\gamma+\Gamma_{\gamma'}}{2}\hat{\rho}_{\gamma,\gamma'}(\gamma\neq\gamma'),$$

$$[L(\hat{\rho})]_{\gamma,\gamma}=-\Gamma_\gamma\hat{\rho}_{\gamma,\gamma}+\sum_{\gamma''}\hat{\rho}_{\gamma'',\gamma''}\Gamma_{\gamma''\to\gamma}, \tag{4}$$

where $\Gamma_\gamma=\Gamma^{intra}_\gamma+\Gamma^{rad}_\gamma$, Γ^{intra}_γ is the rate if intraband relaxation of an exciton γ (this relaxation involves both spin and energy), Γ^{rad}_γ is the interband, radiative rate. The latter can be written as $\Gamma^{rad}_\gamma=B_\gamma\Gamma_0$, where $\Gamma_0=1/\tau_0^{rad}$ is the rate of radiative relaxation for the bright heavy-hole exciton in a QD

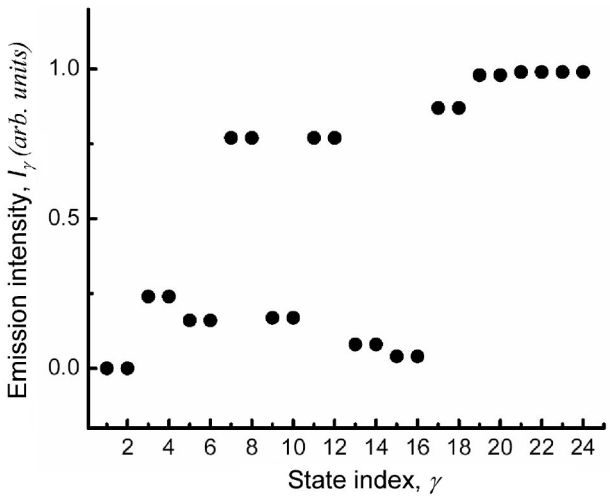

FIG. 2. Emission intensity of exciton with state index γ for the CdTe QD with a single Mn impurity; $R_{Mn}=0$.

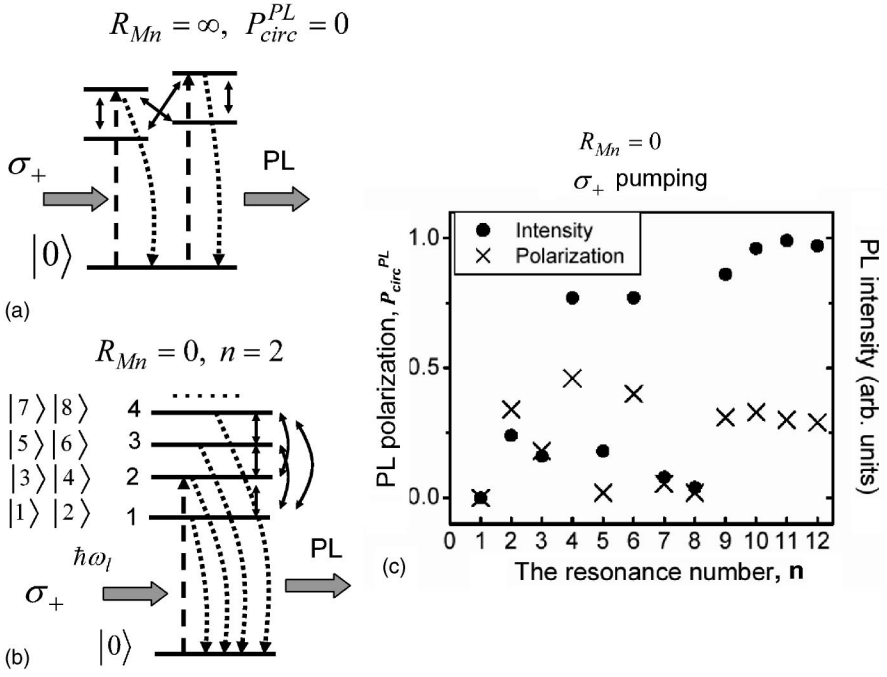

FIG. 3. (a) Exciton spectrum of a QD without a Mn impurity. Arrows show the pumping, emission, and relaxation processes. (b) The pumping and relaxation processes in the presence of a Mn atom; the second level is optically excited, $n=2$ and $\hbar\omega_l=E_3=E_4$. (c) Calculated degree of circular polarization and PL intensity for σ_+ pumping in a QD with $R_{Mn}=0$.

without a Mn impurity; the coefficient B_γ depends on the spin configuration of the exciton.

The long spin relaxation time of paramagnetic ions comes from the spin-lattice interaction.[21] For the Mn relaxation rate in the absence of an exciton, we choose $\Gamma_{Mn}=0.1\ \mathrm{ms}^{-1}$. The intraband relaxation rates $\Gamma_{\gamma\to\gamma'}$ between different momentum and spin states of an exciton depend on a particular system and come from the spin-orbit, electron-phonon, and strong exchange interactions in the conduction and valence bands. In undoped II-VI QD's, the spin relaxation time of an exciton is typically longer that the radiative time. For example, it was found in Ref. 18 that the spin-relaxation time is longer that 0.5 ns. Ref. 20 reports the hole relaxation time is of order of 10 ns. According to the recent time-resolved single-dot study,[19] the spin-relaxation time of exciton can be controlled by the gate voltage in a sample with a metallic back contact. In the voltage-tunable QD's, the spin-relaxation time can be changed in the range 1–10 ns.[19]

For the rate of spin relaxation in the exciton-Mn complex, we choose $\Gamma_1=1/5\ \mathrm{ns}=0.2\ \mathrm{ns}^{-1}$, that is of order of the spin-relaxation rate of exciton in a undoped QD. The interaction between the exciton and Mn spin is given by exchange energy which is about 1 meV. It means that once the hole (electron) spin makes spin flip, the Mn spin can be flipped within about 1 ps. Our choice of the spin-flip time in a strongly coupled Mn-exciton complex (5 ns) seems to be reasonable since the spin-relaxation time in a undoped QD can be tuned down to 1 ns.[19] At finite temperature T, the rates $\Gamma_{\gamma\to\gamma'}$ depend on the energy separation $E_{\gamma'\gamma}=E_{\gamma'}-E_\gamma$. Here we will use a simplified model, $\Gamma_{\gamma\to\gamma'}=\Gamma_1$ if $E_{\gamma'\gamma}<0$ and $\Gamma_{\gamma\to\gamma'}=\Gamma_1 e^{-E_{\gamma'\gamma}/k_BT}$ if $E_{\gamma'\gamma}>0$. This model describes also the thermally activated transitions. For the radiative lifetime, we take a typical value $\tau_0^{rad}=0.5$ ns.

It is important to note that the mechanism of Mn-spin manipulation described below is based on the inequality $\Gamma_{Mn}\ll\Gamma_1$. Since the Mn-spin-relaxation time is really very long $1/\Gamma_{Mn}\sim 1-100$ ms, our mechanism of Mn-spin polarization is relatively insensitive to a particular choice of the parameter Γ_1.

If the light intensity in the pulse is relatively low, Eqs. (4) are reduced to a system of rate equations for the diagonal components $\rho_\alpha=\rho_{\alpha,\alpha}$, where α can be an a exciton-Mn state $|\gamma\rangle$ or a state without exciton, $|I_{Mn,z}\rangle$. In the following, we will be solving numerically a system of rate equations for the two cases. As for the equilibrium density matrix, $\rho^0_{I_{Mn,z'},I_{Mn,z}}=1/6$ and otherwise zero.

IV. Circularly polarized optical emission

The emission intensity of a photogenerated exciton γ is proportional to: $I_{\pm,\gamma}=(2\pi/\hbar)\Sigma_{I_{Mn,z}}|\langle I_{Mn,z}|\hat{V}_\pm^{PL}|\gamma\rangle|^2$, where $|\gamma\rangle$ is the initial exciton state, $|I_{Mn,z}\rangle$ are the final states of the system, and $\hat{V}_\pm^{PL}=V_0(\hat{p}_x\mp i\hat{p}_x)$ are the operators for the photon emission in the direction $+z$. The emission intensity of a given exciton $I_\gamma=I_{+,\gamma}+I_{-,\gamma}$ strongly depends on the state index γ ($\gamma=1,2,\ldots,24$). Some of the excitons are formed mostly of dark states and have low intensity (Fig. 2). Then, the degree of circular polarization of a given exciton state γ can be calculated as $P_{circ,\gamma}=(I_{+,\gamma}-I_{-,\gamma})/(I_{+,\gamma}+I_{-,\gamma})$. In the limit $R_{Mn}\to\infty$ ($A_{e(h)}\to 0$), the exciton wave functions are determined by the anisotropic e-hole exchange interaction, the emission spectrum is linearly polarized,[15] and $P_{circ,\gamma}=0$. For small R_{Mn}, the calculated degrees $P_{circ,\gamma}$ for excitons in a CdTe QD are close to ± 1 because $A_h>a_i,b_i$. Therefore the Mn-related symmetric exchange interaction for small R_{Mn} determines the optical response of excitons.

Since individual excitons have a nonzero degree of circular polarization, PL can also be circularly polarized under the circularly polarized pumping. We now consider the resonant σ_+-optical pumping of CdTe QD into a given pair of states with the energy E_γ ($\hbar\omega_l=E_\gamma$) [Fig. 3(b)]. Also, we assume a

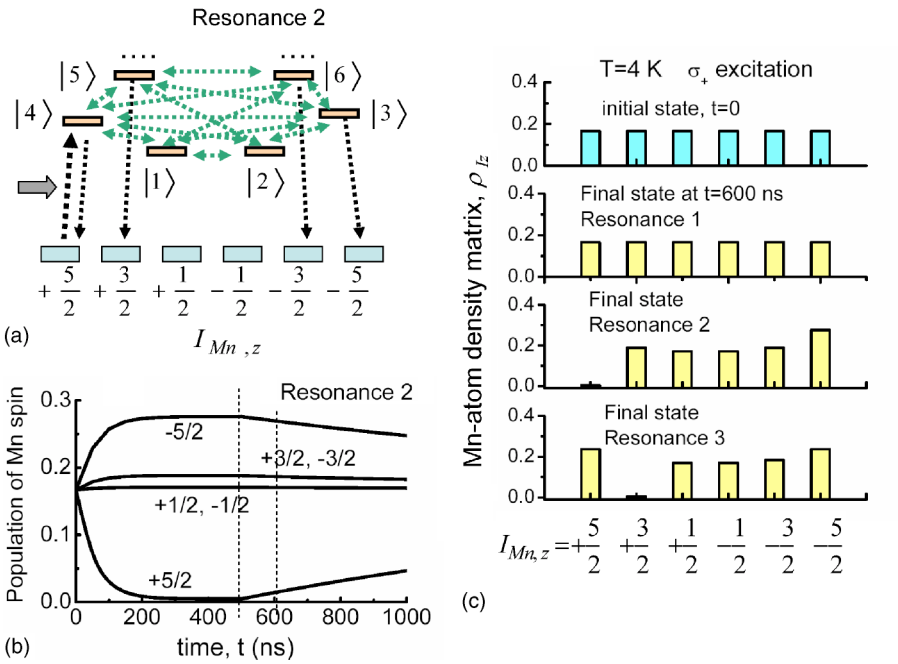

FIG. 4. (a) Schematics of pumping, relaxation, and PL processes in a QD with Mn atom; the second level is resonantly excited $\hbar\omega_l = E_4 = E_3$; here we show only six lowest states. (b) Calculated population of Mn atom states as a function of time for the pulse $\Delta t = 0.5\ \mu$s. Dashed lines indicate the end of pulse and the measurement time. (c) Population of Mn spin states at $t = 0.6\ \mu$s for different resonant pumping. The initial spin state of Mn is randomized.

short laser pulse with a duration $\Delta t \ll \tau_{rad}$. The integrated PL intensity of a QD is given by the diagonal components of the density matrix: $I_{PL,\pm} = \int dt(\Sigma_\gamma \rho_{\gamma,\gamma} \Gamma_\gamma^{PL,\pm})$, where $\Gamma_\gamma^{PL,\pm}$ are the probabilities to emit $\pm$ photons in the vertical direction.

In the limit $R_{Mn} \to \infty$, the upper bright states can be pumped optically [Fig. 3(a)]. Since the individual excitons are linearly polarized, the degree of circular polarization $[P_{circ}^{PL}(\hbar\omega_l = E_\gamma) = (I_{PL,+} - I_{PL,-})/(I_{PL,+} + I_{PL,-})]$ is zero.

In the case of $R_{Mn} < \infty$, the time-integrated PL signal becomes polarized. In Fig. 3, we show the time-integrated PL intensity $I_{PL} = I_{PL,+} + I_{PL,-}$ and P_{circ}^{PL} for all resonant excitations $n = 1, 2, \ldots 12$. The resonance number n in Fig. 3(c) is the number of the exciton energy level counting as shown in Fig. 3(b). For example, the resonance $n = 1$ relates to the states $\gamma = 1, 2$, etc. Overall, the circular polarization of PL under circular pumping is well expressed. The circular polarized PL signal was recently recorded in semimagnetic CdTe QD's.[11] This observation is in contrast to the previous studies of undoped II–VI and III–V QD's.[15] Our theory suggests a qualitative explanation for this observation.

V. Optical writing and manipulation of the Mn spin

We now calculate the time evolution of Mn spin in the presence of and after a long σ_+ pulse of small intensity ($\Delta t = 0.5\ \mu$s, $P_{cv}^2 W_0^2/\hbar^2\Gamma_{rad}^2 = 0.02$). In the initial state at $t = 0$, the Mn atom is in thermal equilibrium, $\rho_{I_{Mn,z}} = 1/6$. The evolution of Mn spin strongly depends on how the QD is pumped. As an example, consider the resonance $n = 2$ ($\hbar\omega_l = E_3 = E_4$) and pumping into the exciton states $|3\rangle$ and $|4\rangle$ [Figs. 4(a) and 4(b)]. The states $|3\rangle$ and $|4\rangle$ optically couple mostly with the Mn states $I_{Mn,z} = \pm 5/2$. Therefore the σ_+ pulse affects mostly the Mn spin state $I_{Mn,z} = 5/2$. We see that, with increasing time, the probability $\rho_{I_{+5/2}}$ decreases, while $\rho_{I_{-5/2}}$ increases. In this process, the σ_+ pulse excites the state $|4\rangle$, then the exciton $|4\rangle$ makes transition to the state $|3\rangle$, and finally the exciton $|3\rangle$ recombines, contributing to the Mn state $I_{Mn,z} = -5/2$. Figure 4 shows the Mn state at the "measurement" time $t = 0.6\ \mu$s. In this way, the Mn spin population becomes nonequilibrium. The exciton ground states $|1\rangle$ and $|2\rangle$ are mostly dark and do not play an important role; they trap and release excitons to the upper energy levels at final T.

The optical probing (*reading*) of the state of Mn atom in a QD can be made with the absorption or PLE single-dot spectroscopies which are presently available.[22] The absorption spectrum of a QD is very sensitive to the Mn spin state.[12,13] For the $\sigma_\pm$ photons with energy $E_3 = E_4$ ($n = 2$), the light absorption intensity is mostly proportional to $\rho_{I_{\pm 5/2}}$ and thus the change in $\rho_{I_{\pm 5/2}}$ can be recorded.

The nonequilibrium spin distribution $\rho_{I_{Mn}}$ strongly depends on the resonance pumping. The resonant pumping into the ground states $|1\rangle$ and $|2\rangle$ is not efficient since these states

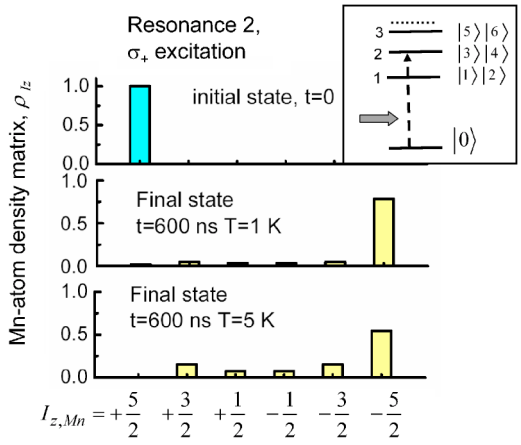

FIG. 5. Population of Mn spin states at $t = 0.6\ \mu$s for the resonant pumping into the second level (inset) at different temperatures. The initial spin state of Mn is +5/2.

are mostly dark [Fig. 4(c)]. The resonant pumping $n=3$ [Fig. 4(c)] results in a remarkable decrease of $\rho_{I_{+3/2}}$ and an increase of $\rho_{I_{-3/2}}$. Simultaneously, the population of the states $I_{Mn,z}=\pm 5/2$ increases. By using proper resonances, most of the spin Mn states can be addressed in this way.

The Mn spin can be prepared in a given initial state using the following optical method. Consider now weak nonresonant illumination of the QD and assume that the QD emits a σ_+ photon with the energy E_4 at $t=0$. According to the selection rules, the emission process projects the QD mostly to the Mn state $I_{Mn,z}=+5/2$. The probability to find the QD after the emission in any other Mn state is much smaller than unity. The state $I_{Mn,z}=+5/2$ can then be used as an initial state in our scheme with the polarized laser pulse started at $t=0$. In the presence of the laser pulse, the Mn state $I_{Mn,z}=+5/2$ turns into the state $I_{Mn,z}=-5/2$ (Fig. 5). At the measurement time $t=0.6$ μs, the Mn spin is mostly in the state $I_{Mn,z}=-5/2$. The temperature effect leads to the mixing with other exciton states and more Mn spin states become involved (Fig. 5). For the qubit operation in this particular QD, it is logical to choose the Mn spin states $\pm 5/2$ and the resonance E_4 ($n=2$) since, for this case, the mixing with the other Mn states is minimum. The preparation of qubit in the state $I_{Mn,z}=+5/2$ can be done by detecting a σ_+ photon with the energy E_4. Then, the process $+5/2 \rightarrow -5/2$ can be realized with a polarized laser pulse. The limiting factors are finite temperature and anisotropic electron-hole exchange interaction which create mixing between the qubit and the other states of the Mn spin. The next logical step is to involve two Mn atoms and consider a two-qubit regime.

To conclude, we have studied the optical properties of the spin state of a single magnetic impurity embedded into a semiconductor QD. It is shown that the Mn impurity can be optically manipulated and the impurity spin can act as a qubit.

ACKNOWLEDGMENTS

One of the authors (A.O.G.) would like to thank Pierre Petroff for motivating discussions. This work was supported by Ohio University, and Volkswagen, and AvH Foundations.

[1] G. A. Prinz, Science **282**, 1660 (1998); S. A. Wolf, D. D. Awschalom, R. A. Buhrman, J. M. Daughton, S. von Molnar, M. L. Roukes, A. Y. Chtchelkanova, and D. M. Treger, *ibid.* **294**, 1488 (2001).

[2] D. Loss and D. P. DiVincenzo, Phys. Rev. A **57**, 120 (1998).

[3] J. K. Furdyna, J. Appl. Phys. **65**, 29 (1988).

[4] *Optical Orientation*, edited by F. Meier and B. P. Zakharchenya (North-Holland, Amsterdam, 1984).

[5] J. M. Kikkawa and D. D. Awschalom, Science **287**, 473 (2000).

[6] I. A. Merkulov, D. R. Yakovlev, A. Keller, W. Ossau, J. Geurts, A. Waag, G. Landwehr, G. Karczewski, T. Wojtowicz, and J. Kossut, Phys. Rev. Lett. **83**, 1431 (1999).

[7] H. Krenn, K. Kaltenegger, T. Dietl, J. Spalek, and G. Bauer, Phys. Rev. B **39**, 109 18 (1989); D. D. Awschalom, J. Warnock, and S. von Molnar, Phys. Rev. Lett. **58**, 812 (1987); T. Dietl, P. Peyla, W. Grieshaber, and Y. Merle d'Aubigne, *ibid.* **74**, 474 (1995).

[8] J. M. Kikkawa, J. J. Baumberg, D. D. Awschalom, D. Leonard, and P. M. Petroff, Phys. Rev. B **50**, 2003 (1994).

[9] P. S. Dorozhkin, A. V. Chernenko, V. D. Kulakovskii, A. S. Brichkin, A. A. Maksimov, H. Schoemig, G. Bacher, A. Forchel, S. Lee, M. Dobrowolska, and J. K. Furdyna, Phys. Rev. B **68**, 195313 (2003).

[10] J. Seufert, G. Bacher, M. Scheibner, A. Forchel, S. Lee, M. Dobrowolska, and J. K. Furdyna, Phys. Rev. Lett. **88**, 027402 (2002).

[11] S. Mackowski, T. Gurung, T. A. Nguyen, H. E. Jackson, L. M. Smith, G. Karczewski, and J. Kossut, Appl. Phys. Lett. **84**, 3337 (2004).

[12] D. M. Hoffman, B. K. Meyer, A. I. Ekimov, I. A. Merkulov, Al. L. Efros, M. Rosen, G. Couino, T. Gacoin, and J. P. Boilot, Solid State Commun. **114**, 547 (2000); A. K. Bhattacharjee and J. Perez-Conde, Phys. Rev. B **68**, 045303 (2003).

[13] A. O. Govorov, Phys. Rev. B **70**, 035321 (2004).

[14] E. L. Ivchenko and G. E. Pikus, *Superlattices and Other Heterostructures. Symmetry and Optical Phenomena* (Springer, Berlin, 1997).

[15] V. D. Kulakovskii, G. Bacher, R. Weigand, T. Kummell, A. Forchel, E. Borovitskaya, K. Leonardi, and D. Hommel, Phys. Rev. Lett. **82**, 1780 (1999); M. Bayer, A. Kuther, A. Forchel, A. Gorbunov, V. B. Timofeev, F. Schafer, J. P. Reithmaier, T. L. Reinecke, and S. N. Walck, *ibid.* **82**, 1748 (1999).

[16] R. J. Luyken, A. Lorke, A. O. Govorov, J. P. Kotthaus, G. Medeiros-Ribeiro, and P. M. Petroff, Appl. Phys. Lett. **74**, 2486 (1999).

[17] C. Schulhauser, D. Haft, R. J. Warburton, K. Karrai, A. O. Govorov, A. V. Kalameitsev, A. Chaplik, W. Schoenfeld, J. M. Garcia, and P. M. Petroff, Phys. Rev. B **66**, 193303 (2002).

[18] S. M. Ulrich, S. Strauf, P. Michler, G. Bacher, and A. Forchel, Appl. Phys. Lett. **83**, 1848 (2003).

[19] J. M. Smith, P. A. Dalgarno, R. J. Warburton, A. O. Govorov, K. Karrai, B. Gerardot, and P. M. Petroff (unpublished).

[20] T. Flissikowski, I. A. Akimov, A. Hundt, and F. Henneberger, Phys. Rev. B **68**, 161309(R) (2003).

[21] D. Scalbert, J. Cernogora, and C. Benoit la Guillaume, Solid State Commun. **66**, 571 (1988).

[22] J. R. Guest, T. H. Stievater, X. Li, J. Cheng, D. G. Steel, D. Gammon, D. S. Katzer, D. Park, C. Ell, A. Thranhardt, G. Khitrova, and H. M. Gibbs, Phys. Rev. B **65**, 241310(R) (2002); B. Alen, F. Bickel, K. Karrai, R. J. Warburton, and P. M. Petroff, Appl. Phys. Lett. **83**, 2235 (2003).